Measurements of the spin-rotation parameters for $\vec{p}d \rightarrow \vec{p}d$ elastic scattering at 496, 647, and 800 MeV

Sun Tsu-hsun,* B. E. Bonner, M. W. McNaughton, H. Ohnuma,† and O. B. van Dyck
Los Alamos National Laboratory, Los Alamos, New Mexico 87545

G. S. Weston, B. Aas, E. Bleszynski, M. Bleszynski, and G. J. Igo
University of California, Los Angeles, California 90024

D. J. Cremans, C. L. Hollas, K. H. McNaughton, P. J. Riley, R. F. Rodebaugh, and Shen-wu Xu
University of Texas, Austin, Texas 78712

S. E. Turpin
Rice University, Houston, Texas 77251

(Received 5 December 1983; revised manuscript received 4 September 1984)

The spin-rotation parameters D_{NN}, D_{SS}, D_{LS}, D_{SL}, and D_{LL}; induced polarization P; and vector analyzing power A at 496 and 647 MeV and D_{SL} and D_{LL} at 800 MeV for p-d elastic scattering have been measured using a polarized proton beam. This work represents the first measurement of the final state L component parameters D_{SL} and D_{LL} for p-d elastic scattering. Comparison with the noneikonal multiple scattering theory reveals large discrepancies between the data and current theory at 800 and 650 MeV but fairly good agreement is seen at 500 MeV. The data also provide for a test of time-reversal invariance.

I. INTRODUCTION

In the last fifteen years there has been a great deal of theoretical and experimental activity concerning nucleon-deuteron scattering at medium energy. Nucleon-deuteron scattering certainly offers the simplest example of a few-body collision. One of the basic motivations of the experimental studies for this process is to investigate whether or not the three-nucleon observables are describable in terms of the known free-NN amplitudes. If so, one can use this fact to extract the information on the NN interaction for cases where these amplitudes are not well determined.

The status of proton-deuteron elastic scattering at medium energies has been reviewed by several authors.[1–4] Coleman *et al.*[5] and Bennett *et al.*[6] made differential cross section measurements of p-d elastic scattering in the intermediate energy region, at 1 GeV, in 1967. Their experiments (unpolarized differential cross section only) were well described by the Glauber multiple-scattering theory after the role of the deuteron D state was understood.[7] Since then the differential cross sections of p-d elastic scattering have been measured over a wide energy range from 316 MeV to 5.73 GeV.[5–6,8–13]

More recently, extensive analyzing power measurements have been made. These data are very helpful, since the study of polarization observables in the elastic scattering of protons from few-body systems is rather sensitive to nucleon-nucleon correlations, Δ intermediate states, and noneikonal propagation. These data now complement the existing differential cross-section data between 200 MeV and 1 GeV.[8–10,13–17]

For forward angles, where the momentum transfer is not too large [$-t \leq 1.2$ (GeV/c)^2], a recent extension[18] of the Glauber multiple-scattering theory with the noneikonal approximation has successfully confronted a considerable amount of p-d elastic scattering data, which include unpolarized differential cross sections[13] and deuteron vector and tensor analyzing power measurements.[16] The tensor analyzing power data in particular provide a sensitive means of revealing deviations from the eikonal approximation due to the presence of the D state in the deuteron wave function. The inclusion of noneikonal corrections in the Glauber diffraction theory is essential, especially for $-t \geq 0.2$ (GeV/c)^2, where discrepancies of up to 150% are observed with theory based on the eikonal approximation. Remarkably good agreement between theory and experiment is obtained for these observables.

Another crucial test of the noneikonal multiple-scattering theory[18,19] is the measurement of the spin-rotation parameters. A complete set of the triple-scattering observables may provide selective information on the p-d collision matrix and, particularly, information on the double spin-flip NN amplitudes. To give a perspective, we present a brief review of the fully spin-dependent, noneikonal formulation of the multiple-scattering theory developed in Ref. 18.

In Ref. 19 it has been pointed out that measurement of the laboratory spin-rotation parameters $D_{NN}(\equiv D)$, $D_{SS}(\equiv R)$, $D_{LS}(\equiv A)$, $D_{LL}(\equiv A')$, and $D_{SL}(\equiv R')$ for $\vec{p}d \rightarrow \vec{p}d$ elastic scattering can be used to determine the depolarization parameters D_0, D_x, D_y, and D_z (D, R, A, A', and R' parameters are the notation of Wolfenstein[20]). In the laboratory system, the initial proton spin direction $\hat{L}$ is defined along $\mathbf{K}_i$, $\hat{N}$ along $\mathbf{K}_i \times \mathbf{K}_f$, and $\hat{S} = \hat{N} \times \hat{L}$; the final proton spin direction $\hat{L}$ is defined along $\mathbf{K}_f$, $\hat{N}$ along $\mathbf{K}_i \times \mathbf{K}_f$, and $\hat{S} = \hat{N} \times \hat{L}$. $\mathbf{K}_i$ and $\mathbf{K}_f$ are the

incident- and scattered-proton momenta in the laboratory system.

In the center-of-mass system, the spin-rotation parameters can be expressed as

$$I_0 D_{\alpha\beta} = \mathrm{Tr}(\sigma_\alpha F \sigma_\beta F^\dagger) , \tag{1}$$

where I_0 is the unpolarized differential cross section,

$$I_0 = \mathrm{Tr}(FF^+) . \tag{2}$$

The depolarization parameters are defined as

$$D_j = \mathrm{Tr}(F_j^\dagger F_j)/I_0 \quad (j=0,x,y,z) , \tag{3}$$

where unit vectors α and β denote the initial and final proton spin directions given by

$$\hat{\mathbf{l}} = (\mathbf{k}_i + \mathbf{k}_f)/|\mathbf{k}_i + \mathbf{k}_f| ,$$
$$\hat{\mathbf{n}} = (\mathbf{k}_i \times \mathbf{k}_f)/|\mathbf{k}_i \times \mathbf{k}_f| ,$$

and

$$\hat{\mathbf{s}} = \hat{\mathbf{n}} \times \hat{\mathbf{l}} .$$

and $\mathbf{k}_f$ are the incident- and scattered-proton momenta in the center-of-mass sytem. The coordinates $\hat{\mathbf{x}}$, $\hat{\mathbf{y}}$, and $\hat{\mathbf{z}}$ are parallel to $\hat{\mathbf{s}}$, $\hat{\mathbf{n}}$, and $\hat{\mathbf{l}}$, respectively. Here, F is the pd collision matrix, which can be written in the general form,

$$F = F_0\sigma_0 + F_x\sigma_x + F_y\sigma_y + F_z\sigma_z , \tag{4}$$

where F_0, F_x, F_y, and F_z are the operators acting in the deuteron spin space, which can be further decomposed in terms of the vector and quadrupole spin 1 operators,[18] and the quantities σ_i are the usual proton spin operators.

The calculation in the framework of the multiple-scattering model of Ref. 19 demonstrates that the depolarization parameters D_j are dependent on the components of the NN amplitudes in a very selective way. If the general form of the NN amplitudes is expressed as

$$f^l_{\mathrm{NN}} = \alpha_l(q) + \beta_l(q)\sigma_y^1\sigma_y^2 + i_{\gamma_l}(q)(\sigma_y^1 + \sigma_y^2) + \delta_l(q)\sigma_x^1\sigma_x^2 + \epsilon_l(q)\sigma_z^1\sigma_z^2 , \tag{5}$$

where l=p,n represent pp and pn amplitudes and the single-scattering contributions to D_x and D_z depend only on the double spin-flip components δ_l and ϵ_l, respectively. The double-scattering contributions to D_x and D_z are also very sensitive to δ_l and ϵ_l. Using D_j, one can extract information on δ_l and ϵ_l. This is the reason that it is useful to define the depolarization parameters D_0, D_x, D_y, and D_z.

It is easy to show that the depolarization parameters D_j in the center-of-mass system and in the Breit system can be expressed as a linear combination of the experimental spin-rotation observables in the laboratory system. They have the following form:

$$\begin{aligned}
D_0 &= \tfrac{1}{4}[1 + D_{NN} + \cos(\chi - \chi')(D_{SS} + D_{LL}) \\
&\quad + \sin(\chi - \chi')(D_{SL} - D_{LS})] , \\
D_x &= \tfrac{1}{4}[1 - D_{NN} + \cos(\chi + \chi')(D_{SS} - D_{LL}) \\
&\quad - \sin(\chi + \chi')(D_{SL} + D_{LS})] , \\
D_y &= \tfrac{1}{4}[1 + D_{NN} - \cos(\chi - \chi')(D_{SS} + D_{LL}) \\
&\quad - \sin(\chi - \chi')(D_{SL} - D_{LS})] , \\
D_z &= \tfrac{1}{4}[1 - D_{NN} - \cos(\chi + \chi')(D_{SS} - D_{LL}) \\
&\quad + \sin(\chi + \chi')(D_{SL} + D_{LS})] ,
\end{aligned} \tag{6}$$

where, in the center-of-mass system,

$$\chi = \frac{\theta_{\mathrm{c.m.}}}{2}, \quad \chi' = -\frac{\theta_{\mathrm{c.m.}}}{2} + \bar{\theta}_L , \tag{7a}$$

and in the Breit system,

$$\chi = \theta_B + 2\alpha - \bar{\theta}_L, \quad \chi' = \bar{\theta}_L . \tag{7b}$$

$\theta_{\mathrm{c.m.}}$, $\bar{\theta}_L$, and θ_B are the scattering angle of the scattered proton in the center of mass system, the antilaboratory system, and the Breit system, respectively. α is an additional angle. $\bar{\theta}_L$, θ_B, and α are defined in Ref. 18. From Eq. (6) one sees it is worthwhile to make a complete measurement of all the spin-rotation parameters in order to determine the D_j parameters and then to check the approximations used in the Glauber model for the case where the NN amplitudes are well known. After this check we hope to use this model to extract the amplitudes, especially the double spin-flip components for neutron-proton scattering, which are not well determined at energies above 500 MeV.

Another interesting aspect of this work is that the data provide for a test on time reversal invariance (TRI). As we describe in Sec. IV A 1, $\vec{\mathrm{p}}$-d elastic scattering is a good choice for this test.

Rahbar *et al.*,[21,22] have made the first measurements of D_{NN}, D_{SS}, D_{LS}, A, and P for $\vec{\mathrm{p}}$d elastic scattering with 496- and 800-MeV proton beams for angles from 20° to 60° (lab). The momentum transfer range for 496 MeV is $0.265\ (\mathrm{GeV}/c)^2 \le -t \le 0.709\ (\mathrm{GeV}/c)^2$; for 800 MeV it is $0.242\ (\mathrm{GeV}/c)^2 \le -t \le 1.494\ (\mathrm{GeV}/c)^2$. Weston *et al.*[23] have measured all the spin-rotation parameters of $\vec{\mathrm{p}}$d elastic scattering at 800 MeV at smaller momentum transfer, $0.006\ (\mathrm{GeV}/c)^2 \le -t \le 0.460\ (\mathrm{GeV}/c)^2$, or 3°–28° (lab).

In the present work we have measured the spin-rotation parameters D_{NN}, D_{SL}, D_{SS}, D_{LS}, D_{LL}, and P; A for $\vec{\mathrm{p}}$d elastic scattering at 496 and 647 MeV from 30° to 60° (lab angle) [$0.293\ (\mathrm{GeV}/c)^2 \le -t \le 0.883\ (\mathrm{GeV}/c)^2$ for 496 MeV; $0.398\ (\mathrm{GeV}/c)^2 \le -t \le 1.175\ (\mathrm{GeV}/c)^2$ for 647 MeV]; and D_{SL} and D_{LL} at 800 MeV from 20° to 50° (lab angle) [$0.243\ (\mathrm{GeV}/c)^2 \le -t \le 1.152\ (\mathrm{GeV}/c)^2$]. This work improved the counting statistics by a factor of 2 or 3 from the first measurements of D_{NN}, D_{SS}, and D_{LS} at 496 MeV by Rahbar *et al.*,[21,22] and represents the first measurements of the final-state L-component parameters D_{SL} and D_{LL} for $\vec{\mathrm{p}}$d elastic scattering.

II. EXPERIMENTAL DETAILS

The experiment was performed using the external proton beam (EPB) at the Los Alamos Meson Physics Facility (LAMPF). The schematic layout of the experimental setup is shown in Fig. 1. The polarized proton beam with polarization oriented in one of three orthogonal directions $(\hat{\mathbf{S}},\hat{\mathbf{N}},\hat{\mathbf{L}})$ was used to bombard a liquid deuterium (LD_2) target. The scattered particles are detected by a polarimeter (JANUS).[24] The conjugate particles are detected by a multiwire drift chamber (MWDC) $C7$ and a plastic scintillator SC. Elastic events were selected using two-body final state kinematics.

The $\hat{\mathbf{N}}$ and $\hat{\mathbf{S}}$ polarization components of the scattered protons can be measured and analyzed by observing the azimuthal distributions after a second scattering in a carbon analyzing target of the polarimeter (JANUS). The other details of JANUS and the data acquisition system are described in Ref. 24.

The method used to determine the transverse polarization components P'_N and P'_S of the scattered particles is similar to the one which was developed at Schweizerisches Institut für NuklearForschung (SIN).[25] With this method, an event at (θ,ϕ) will or will not be accepted depending on whether or not a scattering at $(\theta,\pi+\phi)$ would be accepted by the apparatus ($\pi+\phi$ test). The angles θ and ϕ are the polar and azimuthal scattering angles in the carbon analyzer. This method eliminates some instrumental asymmetries.

The angular distribution $I(\theta,\phi)$ of protons after rescattering in carbon can be written as

$$I(\theta,\phi)=I_0(\theta)[1+P'_N A_c(\theta)\cos\phi-P'_S A_c(\theta)\sin\phi]A(\theta,\phi)\ , \tag{8}$$

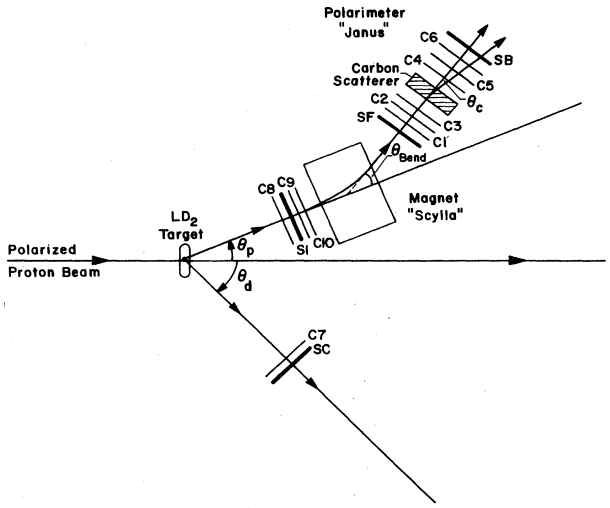

FIG. 1. Schematic layout of the experimental setup.

where I_0 and $A_c(\theta)$ are the corresponding unpolarized differential cross section and analyzing power of the p-^{12}C interaction,[26] and $A(\theta,\phi)$ is the instrumental acceptance function defined by the back scintillator (SB). For the $\phi+\pi$ test, the acceptance function $A(\theta,\phi)$ has periodicity of π, that is,

$$A(\theta,\phi)=A(\theta,\phi+\pi)\ . \tag{9}$$

Using Fourier analysis and then replacing the integrations by sums, for the quantities P'_N and P'_S appearing in Eq. (8), one gets

$$\begin{bmatrix}\sum I(\theta,\phi)A_c(\theta)\cos\phi\\ \sum I(\theta,\phi)A_c(\theta)\sin\phi\end{bmatrix}=\begin{bmatrix}\sum I(\theta,\phi)A_c^2(\theta)\cos^2\phi & \sum I(\theta,\phi)A_c^2(\theta)\cos\phi\sin\phi\\ \sum I(\theta,\phi)A_c^2(\theta)\cos\phi\sin\phi & \sum I(\theta,\phi)A_c^2(\theta)\sin^2\phi\end{bmatrix}\begin{bmatrix}P'_N\\ -P'_S\end{bmatrix}, \tag{10}$$

where the sum goes over all events. The covariance matrix $\tilde{V}(\mathbf{P}')$ of the transverse vector $\mathbf{P}'$, with components P'_N and P'_S, has the following form:

$$\tilde{V}(\mathbf{P}')=\begin{bmatrix}\sum I(\theta,\phi)A_c^2(\theta)\cos^2\phi & \sum I(\theta,\phi)A_c^2(\theta)\cos\phi\sin\phi\\ \sum I(\theta,\phi)A_c^2(\theta)\cos\phi\sin\phi & \sum I(\theta,\phi)A_c^2(\theta)\sin^2\phi\end{bmatrix}^{-1} \tag{11}$$

The statistical uncertainties for P'_N and P'_S are related to $\tilde{V}(\mathbf{P}')$ by

$$\tilde{V}(\mathbf{P}')=\begin{bmatrix}\delta P'^2_N & \delta(P'_N P'_S)\\ \delta(P'_S P'_N) & \delta P'^2_S\end{bmatrix}. \tag{12}$$

For the longitudinal polarization components P'_L of the scattered protons, the measurements are more difficult than for the transverse polarization components. Because of parity conservation one cannot directly measure longitudinal polarization. To solve this problem, a bending magnet is used to precess the spin direction of the scattered particles from L to S, that is, the spin precession angle θ_P is adjusted to be 90°.

The usual relation between precession angle θ_P and bending angle θ_M in the magnet is $\theta_P=1.793\gamma\theta_M$, $\gamma=(1-\beta^2)^{-1/2}$. For various experimental reasons, the average value of θ_P may slightly differ from 90°. Accurate measurement of the average value of θ_P is very important. For example, for the S-spin beam,

$$\frac{P'_S}{P_S}=D_{SL}\sin\theta_P+D_{SS}\cos\theta_P\ , \tag{13}$$

where P_S is the beam polarization. If we want the error of the correction term $D_{SS}\Delta\cos\theta_P$ to be less than 0.01, then the error $\Delta\theta_M$ is required to be less than 0.2°. For the L-spin beam,

$$\frac{P'_L}{P_L}=D_{LL}\sin\theta_P+D_{LS}\cos\theta_P\ , \tag{14}$$

the situation is similar.

To meet the above requirement on θ_P, we set three drift chambers ($C8$, $C9$, and $C10$) and a plastic scintillator detector ($S1$) before the precession magnet (SCYLLA). JANUS was downstream of SCYLLA. The drift chambers ($C8$, $C9$, and $C10$) were well aligned with ($C1$, $C2$, and $C3$) and ($C4$, $C5$, and $C6$) at 0° to keep the geometrical error as small as possible. To clarify the effects of the fringe field of SCYLLA, we measured the average shift of a point on the central axis in the LD_2 target as a function of the magnetic field of SCYLLA by extending the trajectories from ($C8$, $C9$, and $C10$). Then from the data we get an empirical formula for precession angle

$$\theta_P=1.0025\times 1.793\gamma(\theta_M+\Delta\theta)\ ,$$

where $\Delta\theta$ is the actual additional bend angle for each event. By use of this method, the error from the correction due to the D_{SS} component for D_{SL}, and from D_{LS} for D_{LL}, is less than 0.005.

Similarly, small L components in a nominally S-spin beam (or vice versa) are important. These undersirable components were monitored to ±0.5° with the help of a polarimeter in the adjacent line B. (The 46° of precession between the beam lines allows the L components to be measured.) Corrections were made for these undesired components. For the final state S-component data, we have

$$D_{SS}=\frac{1}{P_S}(P'_S-P_L D_{LS})\ , \tag{15}$$

$$D_{LS}=\frac{1}{P_L}(P'_S-P_S D_{SS})\ . \tag{16}$$

The uncertainties due to this correction are less than 0.009. For the final-state L-component data, combining the two corrections mentioned above, we get

$$D_{SL}=\frac{1}{P_L\sin\theta_P}(P'_L-P_S D_{SL}\sin\theta_P -P_S D_{SS}\cos\theta_P-P_L D_{LS}\cos\theta_P)\ , \tag{17}$$

$$D_{LL}=\frac{1}{P_S\sin\theta_P}(P'_S-P_L D_{LL}\sin\theta_P -P_S D_{SS}\cos\theta_P-P_L D_{LS}\cos\theta_P)\ . \tag{18}$$

Usually the term $P_L D_{LS}\cos\theta_P$ for D_{SL} and $P_S D_{SS}\cos\theta_P$ for D_{LL} is negligible. The uncertainties due to the corrections are less than 0.009. The magnitude of the beam polarization was measured using the techniques and calibrations of Ref. 27.

III. EXPERIMENTAL RESULTS

Our results of analyzing power A and induced polarization P for $\vec{p}d\rightarrow\vec{p}d$ elastic scattering at 496 and 647 MeV are given in Figs. 2 and 3. The analyzing power was measured using an N-spin beam. It was calculated using the yields measured with beam spin up and spin down and normalized by the beam intensity as well as the computer live time and efficiency of the detectors.

The induced polarization is the average value of the measured N components from the D_{SS}, D_{LS}, D_{SL}, and D_{LL} measurements. For each measurement we divided the acceptance of the system into three angular bins. The data from these different measurements are all in agreement with each other within the uncertainties.

The spin-rotation parameters D_{NN}, D_{LS}, D_{SL}, D_{SS}, and D_{LL} data for 496 and 647 MeV are shown in Figs. 4 and 5. The D_{SL} and D_{LL} data for 800 MeV are given in Fig. 6. All the parameters are presented as a function of momentum transfer $-t$. The values of all the spin-rotation parameters as well as A and P for 496, 647, and 800 MeV are listed in Tables I–III.

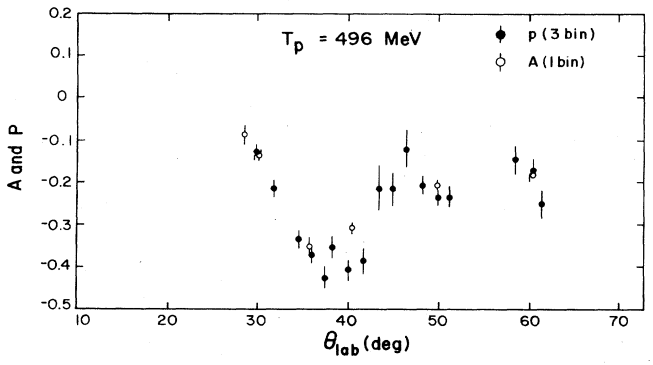

FIG. 2. Analyzing power A and induced polarization P at 496 MeV.

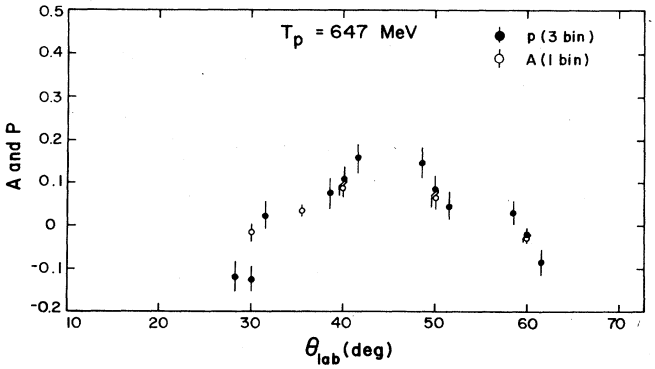

FIG. 3. Analyzing power A for induced polarization P at 647 MeV.

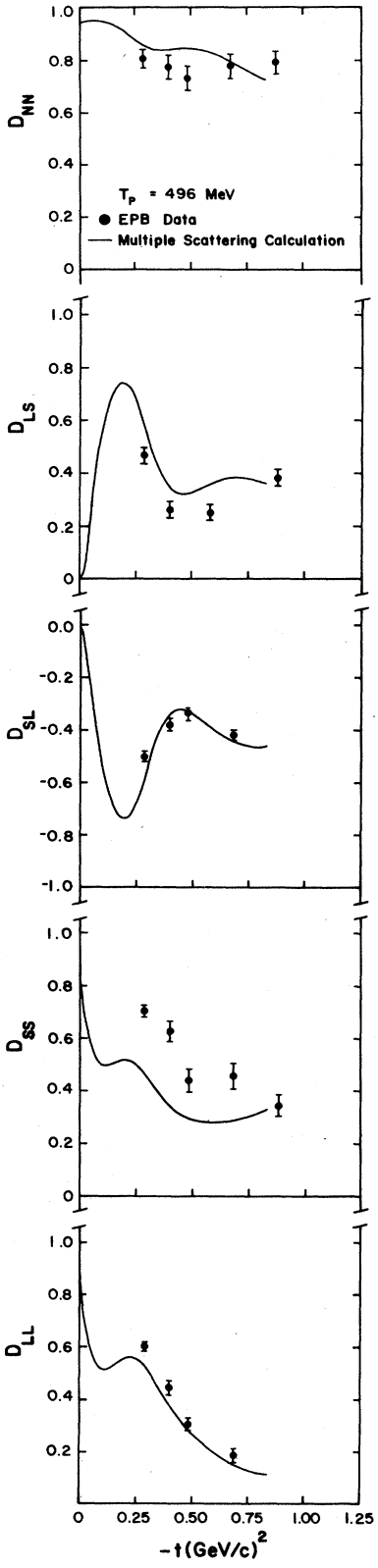

FIG. 4. The data of the spin-rotation parameters at 496 MeV. The theoretical predictions are with energy variation of the NN amplitude.

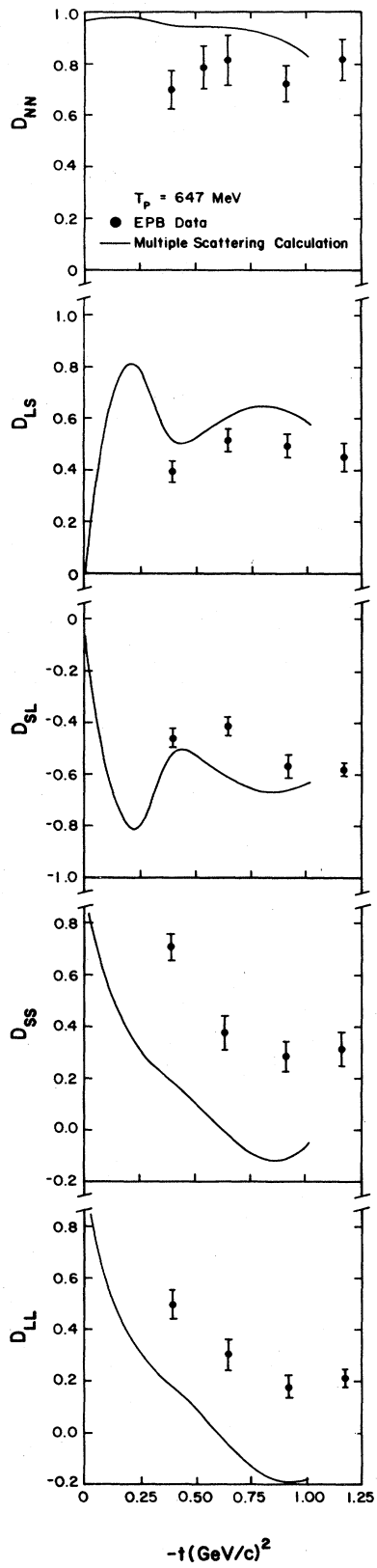

FIG. 5. The data of the spin-rotation parameters for 647 MeV. Curves are as in Fig. 4.

TABLE I. A, P, and $D_{\alpha\beta}$ for 496 MeV.

A		P		D_{NN}	
θ	$A\pm\Delta A$	θ	$P\pm\Delta P$	θ	$D_{NN}\pm\Delta D_{NN}$
30.2°	−0.1638±0.0080	29.9°	−0.1372±0.0087	30.2°	0.8068±0.0348
36.3°	−0.3515±0.0231	36.0°	−0.3988±0.0119	36.3°	0.7732±0.0438
40.5°	−0.3092±0.0131	40.0°	−0.3893±0.0132	40.5°	0.7309±0.0455
50.2°	−0.2092±0.0047	45.2°	−0.1924±0.0239	50.2°	0.7789±0.0445
60.4°	−0.1851±0.0048	50.1°	−0.1985±0.0120	60.4°	0.7920±0.0424
		60.2°	−0.1998±0.0208		

D_{SS}		D_{LS}	
θ	$D_{SS}\pm\Delta D_{SS}$	θ	$D_{LS}\pm\Delta D_{LS}$
30.0°	0.7031±0.0221	30.0°	0.4676±0.0287
36.1°	0.6251±0.0385	36.1°	0.2609±0.0290
40.2°	0.4389±0.0423	45.2°	0.2502±0.0293
50.1°	0.4564±0.0491	60.2°	0.3817±0.0299
60.2°	0.3423±0.0404		

D_{SL}		D_{LL}	
θ	$D_{SL}\pm\Delta D_{SL}$	θ	$D_{LL}\pm\Delta D_{LL}$
29.7°	−0.5004±0.0176	30.0°	0.6027±0.0172
35.9°	−0.3797±0.0227	35.8°	0.4456±0.0267
39.9°	−0.3391±0.0236	40.0°	0.3061±0.0236
50.1°	−0.4171±0.0194	50.2°	0.1850±0.0272

TABLE II. A, P, and $D_{\alpha\beta}$ for 647 MeV.

A		P		D_{NN}	
θ	$A\pm\Delta A$	θ	$P\pm\Delta P$	θ	$D_{NN}\pm\Delta D_{NN}$
29.8°	−0.0142±0.0119	29.9°	−0.0764±0.0180	29.8°	0.6994±0.0740
35.6°	+0.0341±0.0075	39.7°	+0.1149±0.0187	35.6°	0.7858±0.0800
39.8°	+0.0892±0.0217	49.9°	+0.0938±0.0189	39.8°	0.8145±0.0988
49.7°	+0.0617±0.0229	59.7°	−0.0255±0.0148	49.7°	0.7226±0.0692
59.6°	−0.0253±0.0100			59.6°	0.8168±0.0794

D_{SS}		D_{LS}	
θ	$D_{SS}\pm\Delta D_{SS}$	θ	$D_{LS}\pm\Delta D_{LS}$
29.7°	0.7082±0.0493	29.8°	0.3944±0.0394
39.4°	0.3756±0.0647	39.7°	0.5132±0.0451
49.9°	0.2845±0.0560	49.7°	0.4933±0.0431
59.6°	0.3126±0.0644	59.6°	0.4503±0.0554

D_{SL}		D_{LL}	
θ	$D_{SL}\pm\Delta D_{SL}$	θ	$D_{LL}\pm\Delta D_{LL}$
30.0°	−0.4605±0.0369	29.9°	0.4964±0.0528
39.8°	−0.4137±0.0351	39.8°	0.3052±0.0577
50.0°	−0.5685±0.0437	50.0°	0.1778±0.0440
59.8°	−0.5821±0.0260	59.9°	0.2125±0.0329

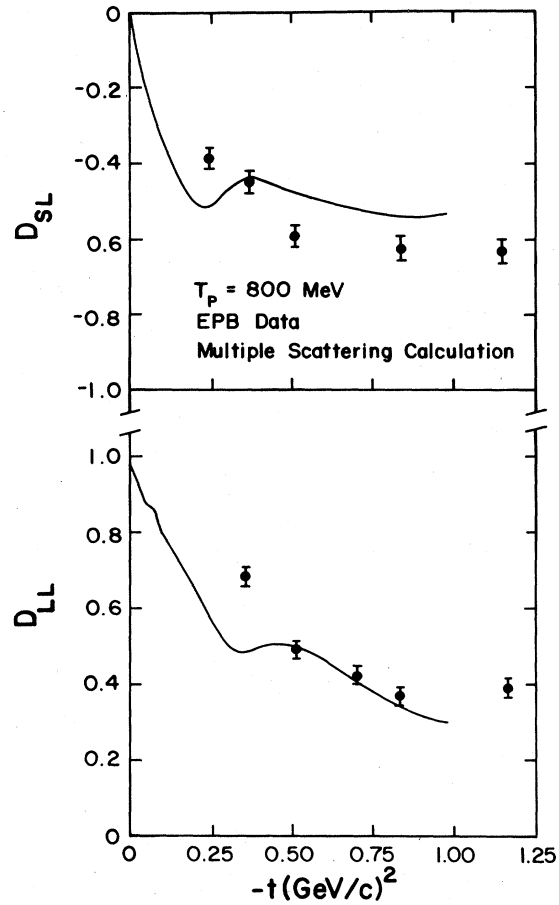

FIG. 6. The data of the spin-rotation parameters D_{SL} and D_{LL} at 800 MeV. Curves are as in Fig. 4.

IV. DISCUSSION AND COMPARISON WITH THEORETICAL PREDICTIONS

A. The test of time-reversal invariance

1. *Comparison of analyzing power and induced polarization*

It is well known that due to TRI the analyzing power $A(\theta)$ observed in the $A(\vec{b},c)D$ reaction is equal to the polarization $P(\theta)$ induced in the $D(c,\vec{b})A$ reaction.[28] Since elastic scattering is its own inverse process, the test of TRI means $A(\theta)=P(\theta)$. But for elastic scattering one must use a target with nonzero spin, because parity conservation alone gives $A(\theta)=P(\theta)$ for a target with zero spin. Furthermore, when the spin-rotation parameter D_{NN} is near unity, the relation $A(\theta)\cong P(\theta)$ will still hold, even if there is a violation of TRI.[29]

In the present work, we have measured D_{NN}, D_{SS}, D_{LS}, D_{SL}, D_{LL}, $A(\theta)$, and $P(\theta)$. As shown in Figs. 4 and 5, D_{NN} is obviously different from unity. So $\vec{p}$-d elastic scattering is a good choice for testing TRI. From Figs. 2 and 3 we see that the relation $A(\theta)\cong P(\theta)$ for 496 and 647 MeV is satisfied within the accuracy of this experiment. There is no evidence for the violation of TRI. More quantitatively we can introduce the value of K for each angle. According to Ref. 22,

$$K=\frac{1-T}{1+T}\ , \tag{19}$$

where T is a TRI violating factor, e.g., $T=1$ or $K=0$ means no TRI violation. It is easy to prove

$$K=\frac{P(\theta)-A(\theta)}{1-D_{NN}}\ . \tag{20}$$

We calculate the value and error of K for each angle and then get the weighted mean $\bar{K}$ and $\Delta\bar{K}$. For 496 MeV data, $\bar{K}\pm\Delta\bar{K}=-0.013\pm0.037$; for 647 MeV data, $\bar{K}\pm\Delta\bar{K}=-0.036\pm0.054$. The results are consistent with the validity of TRI within our accuracy.

2. *Comparison of the spin rotation parameter D_{sl} and D_{ls} in the center-of-mass system*

In the center-of-mass system, the TRI results in the relation

$$D_{sl}=-D_{ls}\ . \tag{21}$$

We can use the following matrix equation to transform the spin-rotation parameters from the laboratory system to the center-of-mass sytem:

$$\begin{bmatrix} D_{ss} \\ D_{ll} \\ D_{ls} \\ D_{sl} \end{bmatrix} = \begin{bmatrix} a & b & -c & -d \\ b & a & d & c \\ c & -d & a & -b \\ d & -c & -b & a \end{bmatrix} \begin{bmatrix} D_{SS} \\ D_{LL} \\ D_{LS} \\ D_{SL} \end{bmatrix} \tag{22}$$

where

TABLE III. D_{SL} and D_{LL} for 800 MeV.

θ	D_{SL} $D_{SL}\pm\Delta D_{SL}$	θ	D_{LL} $D_{LL}\pm\Delta D_{LL}$
19.8°	−0.3858±0.0249	24.5°	0.6824±0.0243
24.7°	−0.4495±0.0306	29.8°	0.4890±0.0231
29.6°	−0.5930±0.0278	35.8°	0.4192±0.0241
39.9°	−0.6257±0.0291	39.8°	0.3661±0.0239
49.3°	−0.6322±0.0304	49.8°	0.3831±0.0231

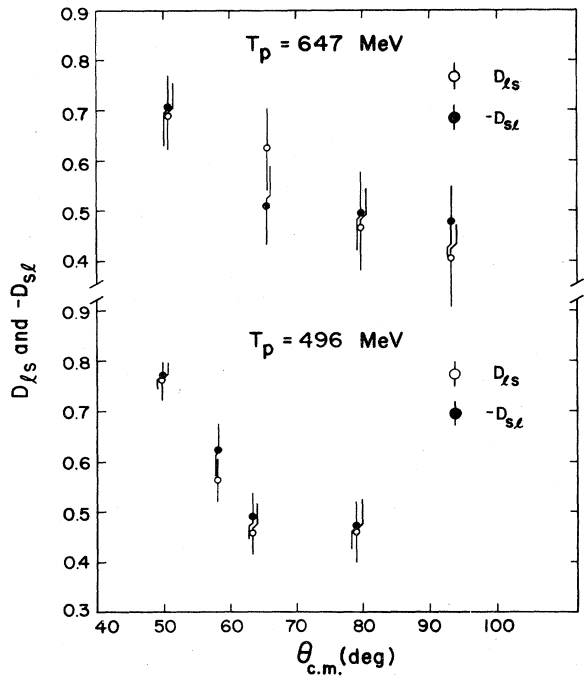

FIG. 7. Comparison between the center of mass system quantities D_{ls} and $-D_{sl}$ at 496 and 647 MeV.

$$
\begin{aligned}
a &= \cos\chi \cos\chi' , \\
b &= \sin\chi \sin\chi' , \\
c &= \sin\chi \cos\chi' , \\
d &= \cos\chi \sin\chi' ,
\end{aligned}
\tag{23}
$$

and χ,χ' as defined in Eq. (7).

For example, for the data at 30° of 496 MeV,

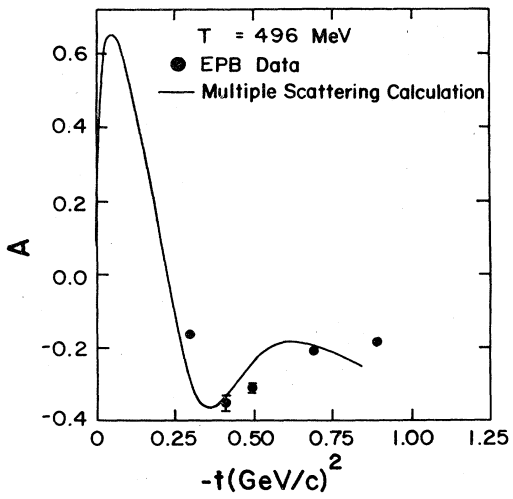

FIG. 8. Comparison between the analyzing power A and the theoretical prediction at 496 MeV. Curves are as in Fig. 4.

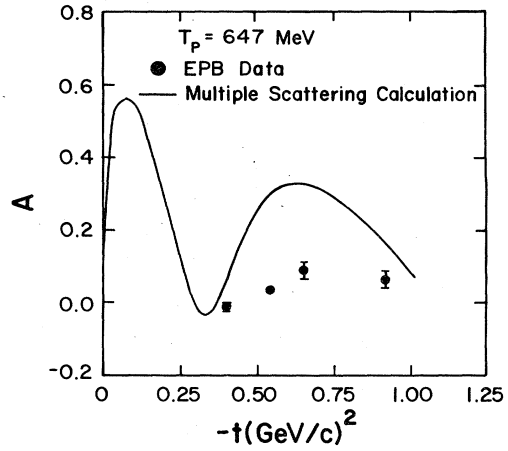

FIG. 9. Comparison between the analyzing power A and the theoretical prediction at 647 MeV. Curves are as in Fig. 4.

$$
\begin{aligned}
D_{ss} &= 0.8966 D_{SS} - 0.0718 D_{LL} - 0.4078 D_{LS} + 0.1578 D_{SL} , \\
D_{ll} &= -0.0718 D_{SS} + 0.8966 D_{LL} - 0.1578 D_{LS} + 0.4078 D_{SL} ,
\end{aligned}
\tag{24}
$$

$$
\begin{aligned}
D_{ls} &= 0.4078 D_{SS} + 0.1578 D_{LL} + 0.8966 D_{LS} + 0.0718 D_{SL} , \\
D_{sl} &= -0.1578 D_{SS} - 0.4078 D_{LL} + 0.0718 D_{LS} + 0.8966 D_{SL} .
\end{aligned}
$$

The spin-rotation parameters in the center-of-mass system are thus seen to be linear combinations of the laboratory quantities. Figure 7 shows the results of D_{ls} and $-D_{sl}$ for 496 and 647 MeV. Within the error bars the relation $D_{ls} = -D_{sl}$ is satisfied. This again indicates the validity of TRI in this experiment.

B. Comparison with the multiple-scattering theory

The theoretical predictions for the spin-rotation parameters obtained in the framework of the multiple-scattering approach of Ref. 19 at 496, 647, and 800 MeV are displayed in Figs. 4–6. In these calculations the p-d elastic-scattering amplitude is given as a sum of the single- and double-collision terms evaluated using the complete spin-dependent NN amplitudes taken from the compilation (*SA*-83) of Arndt *et al.*[30] phase-shift analysis and with the Reid soft-core deuteron wave function. The double-collision term is evaluated with the exact projectile free-wave propagator. In the figures, the solid curve is the calculation including energy variation in the NN amplitudes in the single- and the double-collision terms.

The calculation also shows that in contrast to the tensor observables which have been found to be very strongly affected by the noneikonal propagation effects, these effects do not play a significant role in the observables measured here, because they do not depend very strongly on the deuteron D-wave component.

In order to improve the fit with the data, we have tried alternate sets of NN amplitudes from Dubois,[31] Bugg,[32] and Bystricky.[33] We found in those cases that the devia-

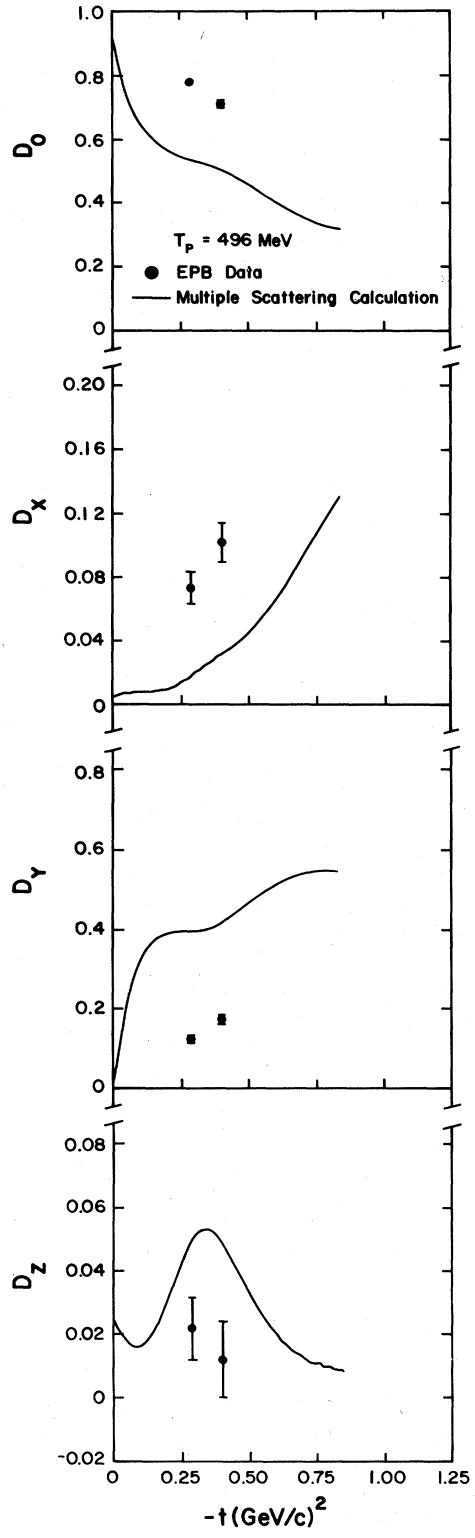

FIG. 10. Comparison between the data of the depolarization parameters D_j in the Breit system and the theoretical prediction for 496 MeV. Solid and dotted curves have the same meaning as in Fig. 4.

tions between the theory and the data are large.

The data of analyzing power A and the theoretical prediction are presented in Figs. 8 and 9 for 496 and 647 MeV. The calculation is in poor agreement with the A_y data.

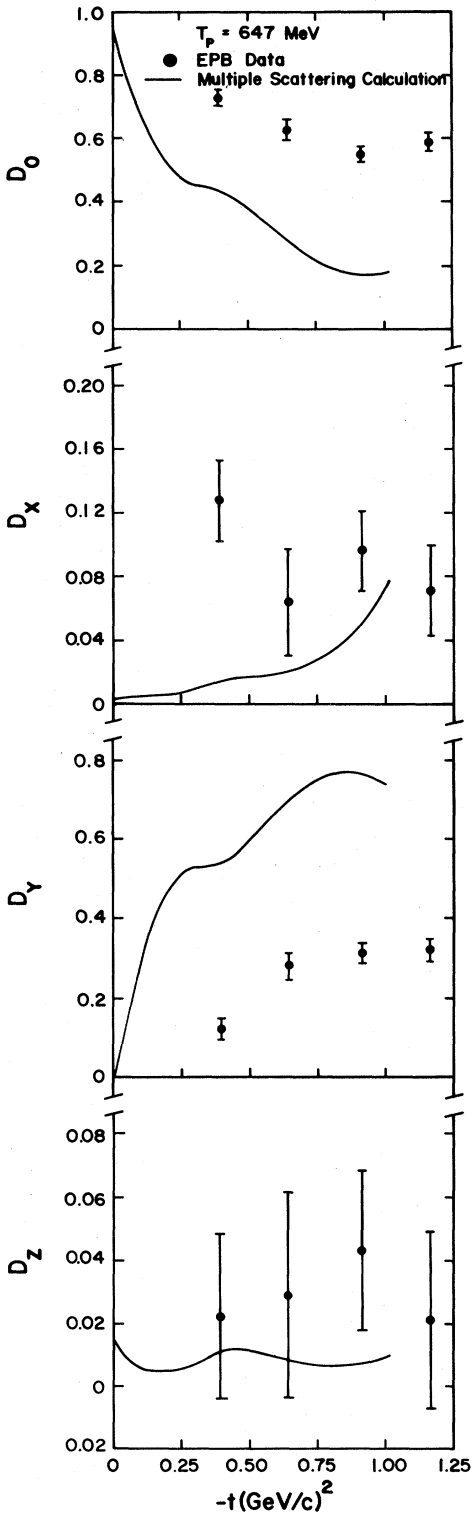

FIG. 11. Same as in Fig. 4 for 647 MeV.

As mentioned in the Introduction, the comparison between the theory and the data of D_j is more transparent and informative than that for the spin rotation parameters. The selective character of D_j, each being related to one component of the p-d collision matrix given by Eq. (3), can be used for tracing the origin of the discrepancies between the theory and the data. For example, if the theory can reproduce D_0, D_x, and D_z, but fails to reproduce D_y, then the problem should result from the amplitude F_y. However, for the spin-rotation parameters, since those are the linear combinations of terms involving all the amplitudes F_j, the failure of the theory upon F_y will be seen in all the spin-rotation parameters.

In the present work, we measured all the spin-rotation parameters. This measurement allows us to extract the depolarization parameters D_j ($j=0$, x, y, z) at 496 and 647 MeV with Eqs. (6) and (7b). D_j are calculated in the Breit system. These are displayed in Figs. 10 and 11 together with the theoretical predictions, where the solid curve has the same meaning as that in Figs. 4—6.

In summary, the discrepancies between current theory and the data are very large at 800 and 650 MeV, as clearly indicated in the data of D_j, but fairly good agreement is seen at 500 MeV. The cause is under investigation. From our analysis for the dependence of the analyzing power on the amplitudes F_j, we found the F_x and F_z are seen to be too small. If these amplitudes were slightly larger, the fit between the theory and the data would be much improved. To clarify this problem, we think it is worthwhile to make a very accurate measurement (uncertainty $\leq 5\%$) of the unpolarized differential cross section for the p-d elastic scattering at the same energy (496 and 647 MeV). That measurement will be most helpful in extracting accurate values of D_x and D_z. We believe that the understanding of the discrepancies presented here is crucial for testing the reaction models for hadron-nucleus scattering at intermediate energies.

ACKNOWLEDGMENTS

One of the authors (T. H. Sun) is much indebted to Dr. Louis Rosen for great hospitality during his stay at LAMPF. This work was supported in part by the Department of Energy.

*On leave from Institute of Atomic Energy, Academia Sinica, Beijing, People's Republic of China.

†Present address: Tokyo Institute of Technology Oh-Okayama, Tokyo 152, Japan.

[1]J. E. Simmons, in *High Energy Physics and Nuclear Structure—1975 (Santa Fe and Los Alamos)*, Proceedings of the Sixth International Conference on High Energy Physics and Nuclear Structure, AIP Conf. Proc. No. 26, edited by D. E. Nagle and A. S. Goldhaber (AIP, New York, 1975), p. 103.

[2]G. Bruge, in Proceedings of the VII International Conference on High Energy Physics and Nuclear Structure, edited by M. P. Locher (Birkhauser, Basel and Stuttgart, 1977), p. 69.

[3]J. M. Cameron, in *Proceedings of the VIII International Conference on High Energy Physics and Nuclear Structure*, edited by D. F. Measday and A. W. Thomas, Nucl. Phys. **A235**, 453 (1980).

[4]G. Igo, in *Proceedings of the IX International Conference on High Energy Physics and Nuclear Structure*, edited by P. Calillon *et al.*, Nucl. Phys. **A374**, 253 (1982).

[5]E. Coleman, R. M. Heinz, O. E. Overseth, and D. E. Pellett, Phys. Rev. Lett. **16**, 761 (1966); E. Coleman, R. M. Heinz, O. E. Overseth, and D. E. Pellett, Phys. Rev. **164**, 1655 (1967).

[6]G. W. Bennett, J. L. Friedes, H. Palevsky, R. J. Sutter, G. J. Igo, W. D. Simpson, G. C. Phillips, R. L. Stearns, and D. M. Corley, Phys. Rev. Lett. **19**, 387 (1967).

[7]D. R. Harrington, Phys. Rev. **176**, 1982 (1968).

[8]N. E. Booth, C. Dolnick, R. J. Esterling, J. Parry, J. Scheid, and D. Sherden, Phys. Rev. C **4**, 1261 (1971).

[9]E. T. Boschitz, W. K. Roberts, J. S. Vincent, M. Blecher, K. Gotow, P. C. Gugelot, C. F. Perdrisat, L. W. Swenson, and J. R. Priest, Phys. Rev. C **6**, 457 (1972).

[10]M. G. Albrow, M. Bonghini, B. Bosnjakovic, F. C. Erné, Y. Kimura, J. P. Lagnaux, J. C. Sens, and F. Udo, Phys. Lett. **35B**, 247 (1971).

[11]L. Dubal, C. K. Hargrove, F. P. Hincks, R. J. McKee, H. Mes, H. C. Thompson, L. Bird, C. H. Halliwell, R. W. Morrison, J. Walters, J. B. McCaslin, and A. R. Smith, Phys. Rev. D **9**, 597 (1974).

[12]J. C. Allder, W. Dellhoff, C. Lunke, C. F. Perdrisat, W. K. Roberts, P. Kitching, G. Moss, W. C. Olsen, and J. R. Priest, Phys. Rev. C **6**, 2010 (1972).

[13]E. Winkelmann, P. R. Bevington, M. W. McNaughton, W. B. Willard, F. H. Cverna, E. P. Chamberlin, and N. S. P. King, Phys. Rev. C **21**, 2535 (1980).

[14]E. Biegert, J. Carroll, W. Dragoset, Jr., R. Klem, J. Lesikar, M. L. Marshak, J. McClelland, T. Mulera, E. A. Peterson, J. B. Roberts, K. Ruddick, R. Talaga, and A. Wriekat, Phys. Rev. Lett. **41**, 1098 (1978).

[15]A. N. Anderson, J. M. Cameron, D. A. Hutcheon, J. Källne, B. K. S. Koene, B. T. Murdock, W. T. H. Van Oers, and A. W. Stetz, Phys. Rev. Lett. **40**, 1553 (1978); Phys. Lett. **87B**, 198 (1979).

[16]M. Bleszynski, J. B. Carroll, M. Haji-Saeid, G. Igo, A. T. M. Wang, A. Sagle, C. L. Morris, R. Kelin, T. Joyce, Y. Makdisi, M. Marshak, B. Mossberg, E. A. Peterson, K. Ruddick, and I. Whittakar, Phys. Lett. **106B**, 42 (1981).

[17]G. J. Igo, M. Bleszynski, J. B. Carrol, A. Sagle, C. L. Morris, R. Klem, T. Joyce, Y. Makdisi, M. Marshak, B. Mossberg, E. A. Peterson, K. Ruddick, and J. Whittakar, Phys. Rev. Lett. **43**, 425 (1979).

[18]G. Alberi, M. Bleszynski, and T. Jaroszewicz, Ann. Phys. (N.Y.) **142**, 299 (1982).

[19]M. Bleszynski, Phys. Lett. **92B**, 91 (1980).

[20]L. Wolfenstein, Phys. Rev. **96**, 1654 (1954).

[21]A. A. Rahbar *et al.* (unpublished).

[22]A. A. Rahbar, Ph.D. thesis, University of California at Los Angeles, Los Alamos Report LA 9505-*T*, 1982.

[23]G. S. Weston, Ph.D thesis, University of California at Los Angeles, Los Alamos Report LA 10174-*T*, 1984.

[24]R. D. Ransome, S. J. Greene, C. L. Hollas, B. E. Bonner, M. W. McNaughton, C. L. Morris, and H. A. Thiessen, Nucl. Instrum. Methods. **201**, 309 (1982).

[25]D. Besset, B. Favier, L. G. Greenious, R. Hess, C. Lechanoine, D. Rapin, and D. W. Werren, Nucl. Instrum.

Methods **166**, 515 (1979).
[26]R. D. Ransome, C. L. Hollas, P. J. Riley, B. E. Bonner, W. D. Cornelius, O. B. van Dyck, E. W. Hoffman, M. W. McNaughton, R. L. York, S. A. Wood, and K. Toshioka, Nucl. Instrum. Methods **201**, 315 (1982).
[27]M. W. McNaughton and E. P. Chamberlin, Phys. Rev. C **24**, 1778 (1981).
[28]R. J. Blin-Stoyle, Proc. Phys. Soc. London **A65**, 452 (1952); G. R. Satchler, Nucl. Phys. **8**, 65 (1958).
[29]H. E. Conzett *et al.*, in *Polarization Phenomena in Nuclear Physics—1980 (Fifth International Symposium, Santa Fe),* Proceedings of the Fifth International Symposium on Polarization Phenomena in Nuclear Physics, AIP Conf. Proc. No. 69, edited by G. G. Ohlson, R. E. Brown, N. Jarmie, M. W. McNaughton, and G. M. Hale (AIP, New York, 1981), p. 1452.
[30]R. A. Arndt, R. H. Hackman, and L. D. Roper, Phys. Rev. C **9**, 555 (1974); **15**, 1002 (1977).
[31]R. Dubois, D. Axen, R. Keeler, M. Comyn, G. A. Ludgate, J. R. Richardson, N. M. Stewart, A. S. Clough, D. V. Bugg, and J. A. Edgington, Nucl. Phys. **A377**, 554 (1982).
[32]D. V. Bugg *et al.*, J. Phys. G **4**, 1025 (1978); Phys. Rev. C **21**, 1004 (1980).
[33]J. Bystricky, E. Lechanoine, and F. Lehar, Saclay Report D.Ph.P.E. 79-01, 1979.